Inorganic Chemistry

Article

pubs.acs.org/IC

Structural Distortions in M[E(SiMe$_3$)$_2$]$_3$ Complexes (M = Group 15, f-Element; E = N, CH): Is Three a Crowd?

Nicholas C. Boyde,[†] Stephen C. Chmely,[†] Timothy P. Hanusa,*[,†] Arnold L. Rheingold,[‡] and William W. Brennessel[§]

[†]Department of Chemistry, Vanderbilt University, Nashville, Tennessee 37235, United States

[‡]University of California, San Diego, La Jolla, California 92093, United States

[§]X-ray Crystallographic Facility, Department of Chemistry, University of Rochester, Rochester, New York 14627, United States

Supporting Information

ABSTRACT: The tris(bistrimethylsilylamido) species P[N(SiMe$_3$)$_2$]$_3$ (**1**) and As[N(SiMe$_3$)$_2$]$_3$ (**2**) have been prepared through halide metathesis in high yield. Their single crystal X-ray structures, along with that of Sb[N(SiMe$_3$)$_2$]$_3$ (**3**), complete the series of structurally authenticated group 15 M[N(SiMe$_3$)$_2$]$_3$ complexes (the bismuth analogue (**4**) has been previously reported). All four complexes possess the expected pyramidal geometries, with progressively longer M−N bond distances from P to Bi but closely similar N−M−N angles (107−104°). The structures of **1**−**4** also display distortions that are similar to those in f-element M[N(SiMe$_3$)$_2$]$_3$ and M[CH(SiMe$_3$)$_2$]$_3$ complexes, in which M···(β-Si−C) interactions have been identified. Such structural features include distorted M−(N,CH)−Si and (N,CH)−Si−C angles and close M···C and M···Si contacts. DFT calculations confirm that there are no M···(β-Si−C) interactions in **1**−**4**; the bond distortions appear to result from the particular steric crowding that arises in pyramidal M[(N,CH)(SiMe$_3$)$_2$]$_3$ complexes. This is likely the source of the most of the distortions in the structures of the f-element analogues as well, even though the latter possess attractive M···Si−C interactions.

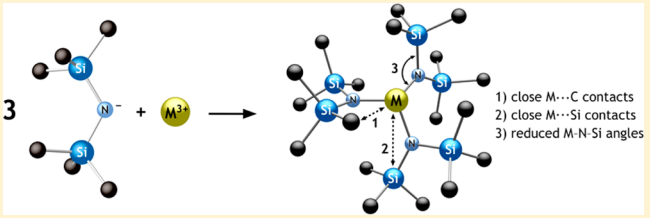

INTRODUCTION

The bis(trimethylsilyl)amido ligand, −N(SiMe$_3$)$_2$, is widely used in metal amide chemistry, owing to the solubility it confers on associated complexes, its substantial steric bulk, and its facile characterization with NMR spectroscopy (^{1}H, ^{13}C, ^{29}Si).[1] It is also compatible with metals from across the periodic table, from group 1 to 16 (including the lanthanides and actinides). Its versatility has led to its incorporation into a variety of precursors for metal−organic chemical vapor deposition (MOCVD) and atomic layer deposition (ALD), and its alkali metal salts are extensively used in synthetic chemistry.[2]

In the course of our work on cyclopentadienyl complexes of the group 15 elements,[3] we had occasion to examine the homoleptic bis(trimethylsilyl)amido complexes as well. Bi[N(SiMe$_3$)$_2$]$_3$ is a long-known compound and has been used to prepare amorphous BiO$_x$ and the ferroelectric perovskite SrBi$_2$Ta$_2$O$_9$.[4] Its crystal structure[4] and some unusual associated reactions[5] have been described. Sb[N(SiMe$_3$)$_2$]$_3$ has been employed in the generation of colloidal InSb nanocrystals,[6] in the preparation of phase-change memory materials,[7] and as a precursor to antimony selenates for thermal pyrolysis studies,[8] although its solid state structure has not been reported. The arsenic complex As[N(SiMe$_3$)$_2$]$_3$ is unknown, but several related heteroleptic compounds have been prepared, including HAs[N(SiMe$_3$)$_2$]$_2$,[9] ClAs[N(SiMe$_3$)$_2$]$_2$,[10] Cl$_2$AsN(SiMe$_3$)$_2$,[11] L$_2$AsN(SiMe$_3$)$_2$ (L = Cr(CO)$_5$, Fe(CO)$_4$),[12] and Cp*AsCl[N(SiMe$_3$)$_2$]$_2$.[13] The tertiary aminophosphine analogue P[N(SiMe$_3$)$_2$]$_3$ is also unknown, but the related hydrogen-bridged dimer {HP[N(SiMe$_3$)$_2$]$_2$}$_2$ has been crystallographically characterized,[9] as have many L$_n$PN(SiMe$_3$)$_2$ derivatives, such as Cl$_2$PN(SiMe$_3$)$_2$,[14] (Me$_3$SiN)$_2$PN(SiMe$_3$)$_2$,[15] and {P[N(SiMe$_3$)$_2$]$_2$}$_4$.[16]

We report here the preparation of P[N(SiMe$_3$)$_2$]$_3$ and As[N(SiMe$_3$)$_2$]$_3$, their single crystal X-ray structures, along with that of Sb[N(SiMe$_3$)$_2$]$_3$, and a comparison of the geometry of the four group 15 M[N(SiMe$_3$)$_2$]$_3$ complexes. During the course of the investigation, it became apparent that many of their geometric features (e.g., distortions in M−N−Si bond angles, close M···C and M···Si contacts) are paralleled in pyramidal f-element M[N(SiMe$_3$)$_2$]$_3$ (and related M[CH(SiMe$_3$)$_2$]$_3$) complexes. Although at one time both agostic M···(γ-H−C) and M···(β-Si−C) interactions (Figure 1) were considered as likely contributors to the f-element structures, continued investigations have demonstrated that M···(γ-H−C) interactions do not contribute to their distinctive geometric features.[17−19]

Complicating this picture is the role of steric effects in agostic and related three-center−two-electron intramolecular interactions.[20] For example, in metal complexes containing bulky

Received: May 26, 2014
Published: August 29, 2014

   dx.doi.org/10.1021/ic501232z | Inorg. Chem. 2014, 53, 9703−9714

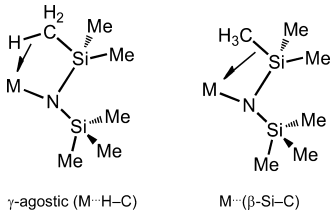

Figure 1. Distinction between attractive agostic (M···H−C) and M···Si−C interactions; only the latter is thought to be operative in $M[(N,CH)(SiMe_3)_2]_3$ complexes.

ligands, a C−H bond may be near a metal because such a location minimizes steric interactions with other ligands; when so positioned, it may engage in an electronic interaction with the metal center.[21] It is conversely possible for steric interactions to place a C−H bond close to a metal center and yet for there to be no agostic interaction, owing to unfavorable orbital energetics (e.g., as with the titanium amide $Ti_2Cl_6[N(t\text{-}Bu)_2]_2$).[22] Although interligand steric stress has been recognized as an influence on the geometries of f-element $M[N(SiMe_3)_2]_3$ and $M[CH(SiMe_3)_2]_3$ complexes, it is generally regarded as playing a secondary role to the M···Si−C interactions.

A basic requirement for a metal center to engage in a delocalized three-center−two-electron interaction is that it be electron-deficient; this accounts for the large number of such complexes among the early transition metals and f-elements. In particular, the existence of energetically accessible d orbitals are thought to be critical to the establishment of M···Si−C interactions.[18] The latter would not normally be expected in the electronically saturated ML_3 complexes of the group 15 elements. Consequently, it was thought that the $M[N(SiMe_3)_2]_3$ complexes described here might serve as a type of experimental "control" in separating the effects of steric crowding (and dispersion forces) from other electronic interactions on the geometries of $M[(N,CH)(SiMe_3)_2]_3$ complexes.

RESULTS AND DISCUSSION

Synthesis. Tris(bistrimethylsilylamido) phosphorus, $P[N(SiMe_3)_2]_3$ (**1**), and arsenic, $As[N(SiMe_3)_2]_3$ (**2**), were synthesized in high yield from salt elimination reactions involving phosphorus trichloride and arsenic triiodide, respectively, and 3 equiv of potassium hexamethyldisilazide in THF or toluene (eq 1):

$$EX_3 + 3\,K[N(SiMe_3)_2] \xrightarrow[-3\,KX]{\text{THF (P); tol (As)}} E\{N(SiMe_3)_2\}_3 \qquad (1)$$

E = P; X = Cl
E = As; X = I

The yellow solids are soluble in polar and nonpolar organic solvents and show no signs of decomposition after 6 weeks in an inert atmosphere at room temperature. The sterically crowded **1** can tolerate limited (ca. 2 h) exposure to air before decomposition is noted. Heating **2** to 100 °C under a static vacuum (10^{-2} Torr) causes decomposition to a brown solid, without evidence of sublimation. This suggests that it probably would have little application in conventional CVD processes, although it might be useful as a synthon for arsenic-containing semiconductors.[23]

Crystallographic Results. *$P[N(SiMe_3)_2]_3$ (**1**).* Crystals of $P[N(SiMe_3)_2]_3$ were isolated from hexane solution as nearly colorless blocks. It crystallizes in the triclinic space group $P\bar{1}$ and is monomeric with three bis(trimethylsilyl)amide ligands arranged around the phosphorus (Figure 2a). Two crystallographically independent molecules are found in the unit cell, as was found for the bismuth analogue;[4] the phosphorus atom is disordered over two sites (in one molecule, in an 80/20 split; in the second, a 77/23 split). The apparent separation between P and P′ is 1.358(3) Å (1.363(2) Å in the second molecule). Owing to the similarity of the two molecules, only the one containing P1 will be discussed here and listed in the tables.

The average P1−N bond length of 1.748(3) Å (1.766(5) Å for P1′−N) is somewhat shorter than that reported for the related compound $\{HP[N(SiMe_3)_2]_2\}_2$ (1.815(14) Å),[9] although the latter contains a four-coordinate P center and might be expected to be slightly lengthened. The P−N bond in the three-coordinate $Cl_2PN(SiMe_3)_2$ (1.6468(8) Å)[14] is even shorter than that in **1**, but this has been attributed to hyperconjugative interaction of the lone pair of the amino nitrogen atom with the antibonding σ^*(P−Cl) bond orbital, leading to partial PN double bond character. A more representative comparison might be with $\{P[\mu\text{-}N(SiMe_3)]PN(SiMe_3)_2\}_2$, in which the terminal three-coordinate PN bond is 1.712 Å in length.[24] The sum of the angles at phosphorus (318.3° at P; 315.8° at P′) reflects the pyramidalization of the molecule. The inclination of the Si−N−Si′ planes to the N_3 plane ranges from 49.6° to 66.5° (average 55.5°); the twist helps to minimize steric interactions.

*$As[N(SiMe_3)_2]_3$ (**2**).* Crystals of $As[N(SiMe_3)_2]_3$ were isolated from hexane solution as nearly colorless blocks. It crystallizes in the monoclinic space group $P2_1/c$ and, like **1**, is monomeric with three bis(trimethylsilyl)amide ligands arranged around the arsenic (Figure 2b). As is found for the other group 15 analogues,[4] the arsenic atom is disordered over two sites (in the case of **2**, in a 55/45 split); the apparent separation between As and As′ is 1.5980(7) Å.

The average As−N bond length of 1.910(3) Å (1.916(2) Å for As′−N) is somewhat longer than that reported for the related compounds $HAs[N(SiMe_3)_2]_2$ (1.878(4) Å),[9] $Cp^*AsCl[N(SiMe_3)_2]_2$ (1.874(2) Å),[13] and $Cl_2As[N(SiMe_3)_2]$ (1.802(3) Å).[11] This could be partly artifactual, stemming from the disorder at the As center, but in fact, the distance is close to that expected from the sum of the covalent radii (1.90 Å).[25] The particularly short As−N bond observed in $Cl_2As[N(SiMe_3)_2]$ has been ascribed to hyperconjugation involving the chlorine atoms, an effect obviously not possible in **2**. The sum of the angles at arsenic (312.0° at As; 310.8° at As′) indicates the substantial pyramidalization present. The Si−N−Si′ planes are inclined at an average angle of 48.1° from the N_3 plane, evidently to minimize steric interactions.

*$Sb[N(SiMe_3)_2]_3$ (**3**).* Compound **3** was found cocrystallized with $HN(SiMe_3)_2$ (see Experimental Section) and is isostructural with **1** and **2**; **3** crystallizes in the trigonal space group $P\bar{3}$, however. It has crystallographically imposed 3-fold symmetry, but like the other $M[N(SiMe_3)_2]_3$ complexes,[4] is disordered over two sites (Figure 2c). The minor contributor could not be as satisfactorily modeled as in the other cases; nevertheless, the major structural features are well-defined.[26]

The Sb−N bond length of 2.100(5) Å matches that expected from the sum of the covalent radii (2.10 Å)[25] and is also identical to that found in the cyclodiphosphazane $[(PN\text{-}t\text{-}Bu)_2(N\text{-}t\text{-}Bu)_2]SbN(SiMe_3)_2$.[27] Sb−N distances in several

dx.doi.org/10.1021/ic501232z | Inorg. Chem. 2014, 53, 9703−9714

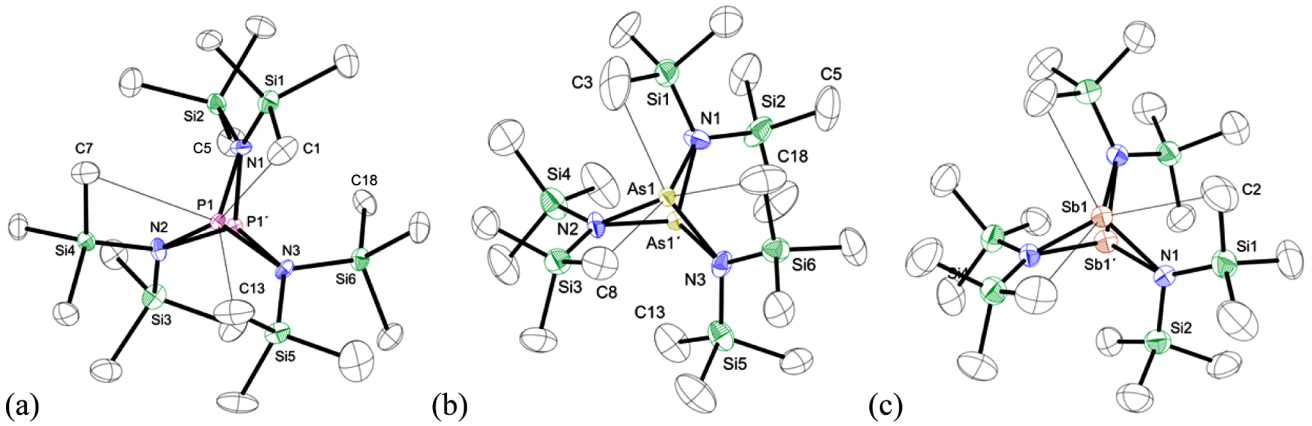

Figure 2. Thermal ellipsoid plot of the non-hydrogen atoms of **1**–**3**, illustrating the numbering scheme used in the text. Thermal ellipsoids are shown at the 50% level. Of the minor conformations, only the M′ atoms are shown. Thin lines are drawn from M to the closest carbon contacts (see text). (a) $P[N(SiMe_3)_2]_3$, selected bond distances (Å) and angles (deg): P1–N1, 1.7427(17); P1–N2, 1.7616(18); P1–N3, 1.7384(17); P1′–N1, 1.807(3); P1′–N2, 1.696(3); P1′–N3, 1.796(3); N1–P1–N2, 106.61(9); N1–P1–N3, 105.08(9); N2–P1–N3, 108.61(9); N1–P1′–N2, 106.63(15); N1–P1′–N3, 100.15(14); N2–P1′–N3, 108.96(15). (b) $As[N(SiMe_3)_2]_3$, selected bond distances (Å) and angles (deg): As1–N1, 1.879(2); As1–N2, 1.896(2); As1–N3, 1.956(3); As1′–N1, 1.917(2); As1′–N2, 1.927(3); As1′–N3, 1.903(3); N1–As1–N2, 105.33(12); N1–As1–N3, 103.71(11); N2–As1–N3, 102.92(12); N1–As1′–N2, 102.70(11); N1–As1′–N3, 104.36(12); N2–As1′–N3, 103.78(11). (c) $Sb[N(SiMe_3)_2]_3$, selected bond distances (Å) and angles (deg): Sb1–N1, 2.100(5); N1–Sb1–N1′, 103.42(19); Si1–N1–Si2, 118.0(2); Sb1–N1–Si1, 108.8(2).

Table 1. Selected Bond Distances (Å) and Angles (deg) and G_{solid} Values (%) in Representative $M[N(SiMe_3)_2]_3$ Complexes[a]

compound	M–N	N–M–N	M···C	M···Si	M–N–Si	N–Si–C	M–N–Si–C	G_{solid}	ref
$Y[N(SiMe_3)_2]_3$	2.224	114.6	2.98	3.18	107.1	108.1	3.1	86.1	69
$Lu[N(SiMe_3)_2]_3$	2.191	111.6	2.89	3.13	104.9	107.2	2.8	86.0	49
$Ce[N(SiMe_3)_2]_3$	2.319	118.2	3.11	3.32	110.4	107.4	7.0	83.6	70
$Nd[N(SiMe_3)_2]_3$	2.290	117.8	3.10	3.29	110.1	108.0	5.8	84.2	71
	2.243	120.0	3.30	3.40	117.7	106.1	10.0	84.4	72
$Sm[N(SiMe_3)_2]_3$	2.284	115.5	3.00	3.24	107.6	107.6	3.9	83.5	18
	2.294	115.1	2.99	3.23	106.8	108.2	3.3	83.4	44
$Tb[N(SiMe_3)_2]_3$	2.333	113.0	2.92	3.18	106.1	107.3	2.0	85.3	73
$Dy[N(SiMe_3)_2]_3$	2.212	114.6	2.97	3.18	107.4	107.8	2.5	84.9	74
$Er[N(SiMe_3)_2]_3$	2.211	113.4	2.94	3.15	106.1	108.8	0.6	84.9	74
$Yb[N(SiMe_3)_2]_3$	2.183	114.5	2.98	3.16	107.4	108.2	2.6	85.6	75
$U[N(SiMe_3)_2]_3$	2.320	116.2	3.04	3.29	108.2	107.7	5.6	81.6	76
$Pu[N(SiMe_3)_2]_3$	2.315	114.0	2.97	3.23	105.9	108.3	3.0	82.7	77
$P[N(SiMe_3)_2]_3$	1.748	106.8	3.14	2.83	106.7	114.2	25.4	92.2	this work
$As[N(SiMe_3)_2]_3$	1.910	104.0	2.95	2.88	103.3	113.7	3.1	89.0	this work
$Sb[N(SiMe_3)_2]_3$	2.100	103.4	3.19	3.15	108.8	112.6	9.9	81.6	this work
$Bi[N(SiMe_3)_2]_3$	2.218	103.7	3.14	3.19	106.6	113.0	4.4	79.1	4

[a]Only the M–N and N–M–N values have been reported for M = Sc and Eu complexes;[78] they have been omitted from this compilation. In molecules with less than C_3 symmetry, average values are cited. M–N–Si, N–Si–C, and M–N–Si–C angles are those nearer the apex of the MN_3 pyramid.

(trimethylsilyl)amido-substituted diazastiboles (2.049(3) and 2.040(3) Å) are only slightly shorter.[28] The sum of the angles at antimony in **3** (310.3°) indicates the considerable pyramidalization in the complex. It should be noted that the angle is substantially wider than that in the tris(amino)stibine $Sb[N(H)(C_6H_2(t\text{-}Bu)_3)]_3$,[29] whose N–Sb–N′ bond angles, which sum to 287.9°, are distorted because of the bulk of the $C_6H_2(t\text{-}Bu)_3$ groups. The heteroleptic complex $(C_6F_5)_2NSb(NEt_2)_2$ has an intramolecular Sb···F interaction that contributes to distortions in the N–Sb–N angles, but they also sum to a value (290.5°) that is considerably less than that in **3**.[30]

Comparison among Group 15 $M[N(SiMe_3)_2]_3$ Derivatives. The ability of the $-N(SiMe_3)_2$ ligand to support isostructural complexes across a broad range of metal sizes is well established (e.g., in the dinuclear series $\{M[N(SiMe_3)_2]_2\}_2$ for M = Mg–Ba[31]). The homoleptic group 15 derivatives are an additional example of this ability. The complexes **1**–**4** are all monomeric pyramidal complexes, and the average M–N bond distances are within 0.03 Å of the sum of the appropriate covalent radii.[25] To a first approximation, the L–M–L′ angles in sets of group 15 ML_3 compounds are expected to become progressively closer to 90° with the heavier complexes, owing to the greater amount of *n*p character in the M–L bonding. Superimposed on this is a trend originating from lessened steric repulsion between the ligands; i.e., angles typically decrease in the order P > As > Sb > Bi, reflecting the longer M–L bonds and consequently reduced interligand interaction in the heavier compounds. Thus, as hydrogen exerts little steric demand, the group 15 hydrides display only small H–M–H variation (93.6°

dx.doi.org/10.1021/ic501232z | Inorg. Chem. 2014, 53, 9703–9714

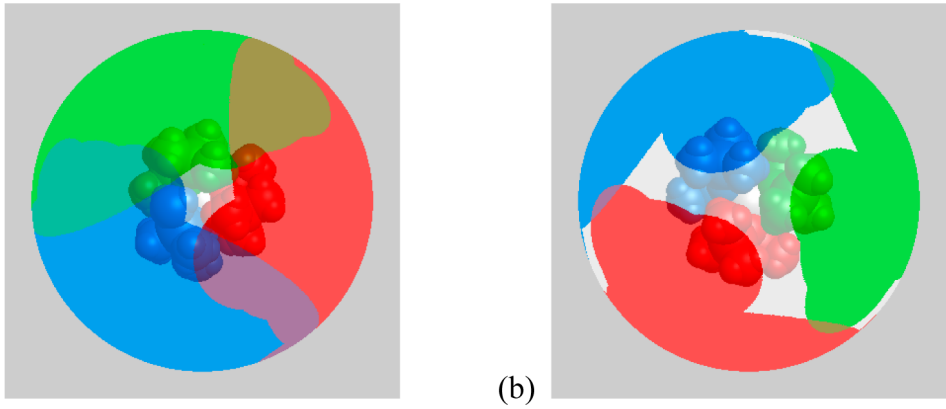

Figure 3. (a) Visualization of the extent of coordination sphere coverage of **1**, using crystallographic coordinates and the program Solid-G.[36] The view is from the bottom of the MN_3 pyramid. (b) The same for the complex $Tb[N(SiMe_3)_2]_3$. The $G_{complex}$ value takes into account the net coverage; regions of the coordination sphere where the projections of the ligands overlap are counted only once.

(PH_3)[32] to 90.5° (BiH_3)[33]), but a larger range is observed in the triphenyls (MPh_3), whose average C−M−C angles decrease from 102.8° (P)[34] to 93.9° (Bi).[35] It is notable that the average N−M−N′ angles in **1**−**4** are both comparatively large (>100°) and exhibit relatively little variation with the change in the central atom (106.8° (P) to 103.7° (Bi)).

The wide N−M−N values in the complexes would appear to be at least partially dictated by steric interactions between the ligands. That these molecules (and their f-element counterparts) are unquestionably crowded species can be visualized through the calculation of their $G_{complex}$ values; this is a measure of the total steric shielding of the metal center by the coordinated ligands.[36] $G_{complex}$ values are listed in Table 1 and depicted in Figure 3 for the two complexes in this study with the shortest (M = P) and longest (M = Tb) M−N bonds; that the values range from 92% to 85% indicates the high percentage of the coordination sphere occupied by the (trimethylsilyl)-amido ligands. More specifically, it can be noted that there are multiple interligand Me···Me′ contacts less than 4.0 Å (the sum of the van der Waals radii[37]) in the complexes; the closest Me···Me′ contact in **2** is at 3.56 Å, in **3** at 3.69 Å, and in **4** at 3.82 Å. Those in **1** are especially close, as short as 3.36 Å (C5−C18).

There are consistently observed distortions in the $-N(SiMe_3)_2$ ligands in the group 15 compounds that are not present in less sterically congested species. For example, in **2**, the As and C3, C8, and C18 atoms are at distances of 2.93, 2.99, and 2.92 Å, respectively; all other carbons are over 3.9 Å from the arsenic (in the related $HAs[N(SiMe_3)_2]_2$,[9] the closest As···C contact is at 3.39 Å). In addition, the As−N−Si angles involving these carbons are 102.8(1)°, 104.8(1)°, and 102.3(1)°, respectively, consistent with the orientation of the carbon atoms toward the arsenic (none of the comparable angles in $HAs[N(SiMe_3)_2]_2$ is less than 117°). The As−N−Si−C torsion angles involving the close carbons in **2** are 3.9° or less. The evidence for similar orientations in **3** and **4** is almost as strong; the closest Sb···C and Bi···C contacts are at 3.19 and 3.13 Å, respectively, for example, and the corresponding M−N−Si angles are 108.8(2)° and 106.1°, respectively. Reflecting the even larger amount of steric crowding in **1**, the pattern of ligand distortions is modestly different from the three heavier complexes. For example, although there is a close P···C contact at 3.08 Å, the P−N−Si−C torsion angle involving that carbon is 13.6°, nearly 10° more than that in **2** (3.9°). In general, however, the pattern of ligand distortions is similar in all four compounds and is comparable to that observed in the complexes of the f-elements (see below).

Bonding and Structure in $M[(N,CH)(SiMe_3)_2]_3$ Complexes. Despite the differences in the regions of the periodic table from which the pyramidal $M[N(SiMe_3)_2]_3$ and related $M[CH(SiMe_3)_2]_3$ complexes originate, they share certain structural features that can be use useful in discussing their bonding.

Absence of M···H−C Agostic Bonding. There are characteristic values for M···H distances (1.8−2.3 Å) and M···H−C angles (90−140°) that can be expected for agostic interactions,[38] but in the available crystal structures of $M[N(SiMe_3)_2]_3$ and $M[CH(SiMe_3)_2]_3$ complexes, hydrogen atoms have been inserted in calculated positions and refined using a riding model. Owing to such constraints on the geometry of the C−H bond, the significance that can be placed on the final M···H distances and M···H−C angles is limited. Nevertheless, in a study of the structure and bonding in $Sm[N(SiMe_3)_2]_3$,[18] a detailed analysis of the metal−ligand geometry led the authors to determine that, despite the existence of short Sm···H contacts, "attractive interactions with the γ-C−H bonds are not present. These interactions are in fact *repulsive*" [italics added]. A similar conclusion was reached for $La[CH(SiMe_3)_2]_3$[17] and the titanium amide $Ti_2Cl_6[N(t\text{-}Bu)_2]_2$,[22] and for the complexes $(C_5Me_5)La[CH(SiMe_3)_2]_2$[39,40] and $(C_5Me_5)Y(OC_6H_3(t\text{-}Bu)_2)[CH(SiMe_3)_2]$,[40] in which neutron diffraction experiments enabled the accurate location and refinement of hydrogen atom positions.

Tellingly, the same arrangements of the central element and ligand hydrogens are present in the group 15 complexes; for example, the hydrogen atoms bound to the γ-carbons of the $[N(SiMe_3)_2]^-$ ligands are oriented so as to *maximize* their distances to the metal center. The dihedral As···Si−C−H angles in **2**, for example, are in the range from 54° to 66°, and not near zero, which would be expected if there were attractive As···H interactions; comparable values are found in the other complexes.

Evidence for M···Si−C Interactions. There are several structural criteria that have been cited as evidence for M···(β-Si−C) interactions in $M[N(SiMe_3)_2]_3$ and $M[CH(SiMe_3)_2]_3$ complexes, including distorted M−(N,CH)−Si and (N,CH)−Si−Me angles, small M−(N,CH)−Si−Me torsion angles (this is less notable with the nonplanar $-CH(SiMe_3)_2$ ligands), elongated Si−Me bonds for the carbon interacting with the

dx.doi.org/10.1021/ic501232z | *Inorg. Chem.* 2014, 53, 9703−9714

Table 2. Selected Bond Distances (Å) and Angles (deg) and G_{solid} Values (%) in Representative $M[CH(SiMe_3)_2]_3$ Complexes[a]

compound	M−C	C−M−C	M···C(H_3)	M···Si	M−C−Si	C−Si−C(H_3)	M−C−Si−C(H_3)	G_{solid}	ref
$Y[CH(SiMe_3)_2]_3$	2.353	108.6	2.96	3.28	102.1	106.6	12.4	85.0	43
	2.357	108.1	2.95	3.28	101.7	106.3	13.1	84.6	42
$La[CH(SiMe_3)_2]_3$	2.516	109.3	3.12	3.41	101.9	109.7	13.9	79.8	79
$Ce[CH(SiMe_3)_2]_3$	2.475	110.1	3.07	3.39	102.8	108.2	11.8	82.0	43
$Sm[CH(SiMe_3)_2]_3$	2.332	110.2	3.04	3.33	106.6	105.2	14.4	84.9	79
$U[CH(SiMe_3)_2]_3$	2.486	107.6	3.10	3.37	101.7	109.5	16.2	82.9	80
$Bi[CH(SiMe_3)_2]_3$	2.328	102.9	3.48	3.40	106.6	113.0	29.0	78.7	81

[a]In molecules with less than C_3 symmetry, average values are cited. M−C−Si, N−Si−C(H_3), and M−C−Si−C(H_3) angles are those nearer the apex of the MC_3 pyramid.

metal, relatively short M···Si contacts, and the placement of one or more of the carbon atoms close (~3 Å) to the metal atom. The existence of these structural features are more reliably established than are the location of hydrogen atoms in X-ray crystal structures, and most are included in the tabulation in Tables 1 (for $M[N(SiMe_3)_2]_3$ complexes) and 2 (for $M[CH(SiMe_3)_2]_3$ complexes).[41] The discussion below will focus primarily on the amido complexes, although similar comments can be made for the alkyl species.

These distortions and contacts are not completely independent. For example, compared with complexes with longer M−N bonds (Figure 4a), those with shorter M−N

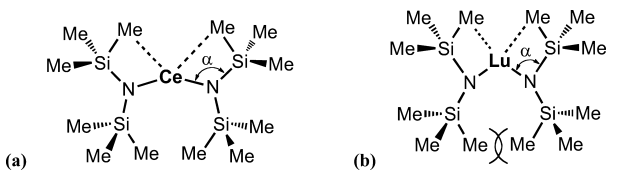

Figure 4. Relationship between various bond distances and intramolecular contacts in $M[N(SiMe_3)_2]_3$ complexes, using Ce and Lu complexes as examples. (a) In $Ce[N(SiMe_3)_2]_3$, the M−N distance is 2.319 Å, the N−Ce−N is 118.2°, and the angle α is 110.4°; the corresponding Ce···C(H_3) contact is at 3.11 Å. (b) In $Lu[N(SiMe_3)_2]_3$, the Lu−N distance is shortened to 2.191 Å; the N−Lu−N angle has narrowed to 111.6°, as has the angle α to 104.9°; the accompanying Lu···C(H_3) contact is now at 2.98 Å.

bonds would be expected to have closer contacts between the basal TMS groups, which would have the effect of tilting the ligands toward the more open apex side of the MN_3 pyramid (Figure 4b). The "upper" M−N−Si angle would thereby be compressed, and the silicon atom (and an attached methyl group) would be pushed closer to the metal.

For the f-element $M[N(SiMe_3)_2]_3$ complexes, there is in fact a strongly linear relationship between the N−M−N angle and the closest M···C(H_3) distance (Figure 5). Interestingly, the comparable angle/distance relationship for the heaviest group 15 complexes falls on a nearly vertical line, owing to the much smaller spread in the N−M−N angles; the highly congested compound **1** falls somewhat off the line of the heavier compounds. Also notable is the lack of strong C(H)−M−C(H) and M−C distance correlation in the f-element $M[CH(SiMe_3)_2]_3$ complexes, perhaps a consequence of the longer M−C vs M−N bond lengths, and an ability of the nonplanar $[CH(SiMe_3)_2]^-$ anion to pack around the metal centers in a way that does not occur for the planar $[N(SiMe_3)_2]^-$ ligand. Perhaps coincidentally, the value for $Bi[CH(SiMe_3)_2]_3$ is on the line observed with the group 15 $M[N(SiMe_3)_2]_3$ complexes.

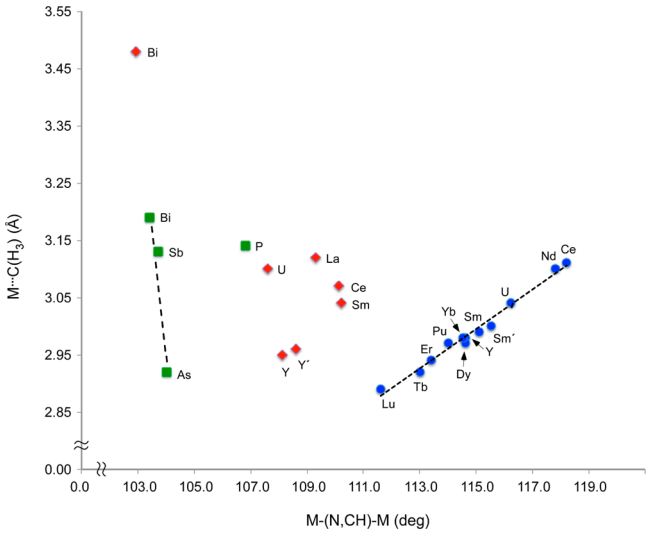

Figure 5. Relationship between (N,CH)−M−(N,CH) angles and closest intramolecular M···C(H_3) contacts in $M[N(SiMe_3)_2]_3$ (M = f-element (blue); group 15 (green)) and $M[CH(SiMe_3)_2]_3$ (red) complexes. The red symbols for Y and Y′ are from refs 42 and 43, respectively; those for the blue Sm and Sm′ are from refs 44 and 18, respectively. The least-squares line drawn for the f-element $M[N(SiMe_3)_2]_3$ complexes has $r^2 = 0.98$; the line for $(As–Bi)[N(SiMe_3)_2]_3$ has $r^2 = 0.91$.

In general, the main-group complexes are more strongly pyramidal than the f-element compounds (average N−M−N of 104.5° and 114.9°, respectively), and the N−Si−C angles average 113.4° for the group 15 compounds but a smaller 107.5° for the f-element counterparts. Given the considerably different M−N bonding in the complexes (largely covalent in the group 15 complexes; much more polar, even if not completely electrostatic, in the f-element counterparts), however, there is a substantial degree of structural similarity between them.

Computational Investigations and Steric Effects. The difference in the electronic nature of the central elements in the $M[N(SiMe_3)_2]_3$ complexes, especially considering the expected lack of energetically relevant acceptor orbitals in **1**−**4**, suggests that intramolecular crowding is a likely source of some of the structural similarities. This is not a completely new proposal; for example, the inequality in the M−(N,CH)−Si angles in the f-element complexes has previously been suggested to be partially the result of steric effects, independent of explicit orbital interactions.[18]

As a starting point in a computational examination of this issue, we used the molecular mechanics force field UFF[45] as a tool to estimate the extent to which the structural features of

dx.doi.org/10.1021/ic501232z | Inorg. Chem. 2014, 53, 9703−9714

Table 3. Selected Experimental and UFF Optimized Bond Distances (Å) and Angles (deg) for $Pu[N(SiMe_3)_2]_3$, $Ce[CH(SiMe_3)_2]_3$, and $Sb[N(SiMe_3)_2]_3$

		$Pu[N(SiMe_3)_2]_3$	$Ce[CH(SiMe_3)_2]_3$	$Sb[N(SiMe_3)_2]_3$
M−(N,CH)	(expt)	2.315(10)	2.475(7)	2.100(5)
	(calcd)	2.287	2.512	2.107
M···Si	(expt)	3.23	3.38	3.15
	(calcd)	3.25	3.39	3.19
M···C	(expt)	2.968(9)	3.068(7)	3.19
	(calcd)	3.04	2.98	3.25
(N,CH)−M−(N,CH)	(expt)	113.97(5)	110.08(16)	103.42(19)
	(calcd)	101.1	104.6	100.8
M−(N,CH)−Si	(expt)	105.9(2)	102.8(3)	108.8(2)
	(calcd)	108.4	100.5	109.4
(N,CH)−Si−C	(expt)	108.3(4)	108.2(4)	112.6(3)
	(calcd)	107.9	105.6	113.4
M−(N,CH)−Si−C	(expt)	3.0	11.8	9.9
	(calcd)	10.0	19.8	9.6

Table 4. Selected Experimental and DFT Optimized Bond Distances (Å) and Angles (deg) for $E[N(SiMe_3)_2]_3$ (E = P−Bi)[a]

		$P[N(SiMe_3)_2]_3$	$As[N(SiMe_3)_2]_3$	$Sb[N(SiMe_3)_2]_3$	$Bi[N(SiMe_3)_2]_3$
M−N	(expt)	1.748(3)	1.910(3)	2.100(5)	2.218(13)
	(calcd w/o *d*)	1.821	1.926	2.099	2.183
	(calcd w/*d*)	1.781	1.913	2.101	2.186
M···Si	(expt)	2.83	2.88	3.15	3.19
	(calcd w/o *d*)	2.95	3.08	3.23	3.29
	(calcd w/*d*)	2.92	3.07	3.23	3.29
M···C	(expt)	3.14	2.95	3.19	3.14
	(calcd w/o *d*)	3.18	3.15	3.25	3.24
	(calcd w/*d*)	3.20	3.15	3.25	3.24
N−M−N	(expt)	106.8(2)	104.0(2)	103.42(19)	103.7(5)
	(calcd w/o *d*)	105.9	103.6	102.2	103.1
	(calcd w/*d*)	106.1	103.5	102.1	103.1
M−N−Si	(expt)	106.7(2)	103.3(2)	108.8(2)	106.6(7)
	(calcd w/o *d*)	109.4	112.1	112.9	112.3
	(calcd w/*d*)	109.3	112.1	112.8	112.2
N−Si−C	(expt)	114.2(2)	113.7(3)	112.6(3)	113.0(1.1)
	(calcd w/o *d*)	111.1	109.8	110.3	109.8
	(calcd w/*d*)	111.8	109.9	110.2	109.6
M−N−Si−C	(expt)	25.4	3.1	9.9	4.4
	(calcd w/o *d*)	26.1	5.9	5.6	2.3
	(calcd w/*d*)	27.6	6.2	5.5	2.1

[a]Basis set for "calcd w/o *d*" is LANL08 (E) and def2SVP (C, H, N, Si); that for "calcd w/*d*" is LANL08(d) (E) and def2SVP (C, H, N, Si).

the $M[(N,CH)(SiMe_3)_2]_3$ complexes might be generated from steric (and dispersion) interactions. $Pu[N(SiMe_3)_2]_3$, $Ce[CH(SiMe_3)_2]_3$, and $Sb[N(SiMe_3)_2]_3$ (**3**) were selected as representative examples for actinide, lanthanide, and group 15 metal centers; Table 3 lists the results.

In general, the distances between directly bonded atoms are more reliably modeled with MM methods than are the corresponding angles, and the M−(N,CH) bond lengths are calculated to be within 0.04 Å of their respective experimental values. The relatively limited parametrization of the heavy metal centers, their low coordination numbers, and, in the case of the amido complexes, the failure of the UFF method to capture M−N π interactions that may be present[46] are perhaps responsible for the overpyramidalization of the (N,CH)−M−(N,CH) angles; the error, not surprisingly, is least with the Sb complex (2.6°). Nevertheless, although possibly benefiting from some error cancellation,[47] the long-range contacts are reasonably well represented; the M···Si and M···C distances are overestimated by a maximum of only 0.04 Å for M···Si (in **3**) and a maximum of 0.09 Å for M···C (in the Ce complex). Considering the approximate nature of the modeling, the structures are represented surprisingly well, especially that of **3**, where the shorter Sb−N bonds and consequently tighter intramolecular packing limits the conformational flexibility of the ligands (note that the M−N−Si−C torsion angle is reproduced to within 0.3° of the experimental value in **3**, whereas in $Ce[CH(SiMe_3)_2]_3$, with the longest metal−ligand bonds of the three compounds, the comparable M−(CH)−Si−C angle deviates by 8.0°).

Although any molecular mechanics representation has substantial limitations, the fact that simply holding three $-(N,CH)(SiMe_3)_2$ groups together around a central metal within the influence of an orbital-free force field can reproduce several of the major features of the complexes suggests that the MM approach is capturing a critical contributor to their structures; that is, steric congestion and van der Waals

dx.doi.org/10.1021/ic501232z | Inorg. Chem. 2014, 53, 9703−9714

Table 5. Percent Mulliken Contribution of Various Atomic Orbitals in the Relevant MOs of Compounds 1−4 and $Lu[N(SiMe_3)_2]_3$

	$P[N(SiMe_3)_2]_3$				$As[N(SiMe_3)_2]_3$			
AO	HOMO	HOMO − 1	HOMO − 2	HOMO − 3	a (LP)	e (LP)	a (σ)	e (σ)
$-E$ (au)	0.155	0.212	0.217	0.222	0.172	0.211	0.234	0.250
M(s)	18.3	1.1	0.0	4.5	10.9	0.0	7.59	0.0
M(p)	28.0	3.7	0.0	10.9	12.6	0.0	19.04	0.68
M(d)	0.0	1.5	1.3	0.0	1.2	0.74	0.0	0.0
N(tot)[a]	38.9	51.3	51.4	37.2	52.9	54.5	25.8	3.6
Si(p)[b]	0.0	0.0	0.0	1.0	0.0	0.0	2.31	12.7
Si(d)[b]	0.0	0.0	1.2	2.8	0.0	1.2	0.0	0.54
	$Sb[N(SiMe_3)_2]_3$				$Bi[N(SiMe_3)_2]_3$			
AO	a (LP)	e (LP)	a (σ)	e (σ)	a (LP)	e (LP)	a (σ)	e (σ)
$-E$ (au)	0.178	0.209	0.228	0.250	0.182	0.209	0.226	0.250
M(s)	14.9	0.0	9.6	0.0	15.8	0.0	9.2	0.0
M(p)	12.3	0.0	20.0	1.8	11.3	0.0	20.3	2.4
M(d)	0.0	0.7	0.0	0.0	0.0	0.6	0.0	0.0
N(tot)[a]	49.0	54.2	26.5	6.3	47.8	54.9	33.1	9.9
Si(p)[b]	0.0	0.0	0.0	11.9	0.0	0.0	0.0	12.1
Si(d)[b]	0.0	0.0	0.0	1.1	0.0	1.8	0.0	0.0

	$Lu[N(SiMe_3)_2]_3$			
AO	a (LP)	e (LP)	e (σ)	a (σ)
$-E$ (au)	0.194	0.203	0.228	0.229
Lu(s)	0.0	0.0	0.0	3.3
Lu(p)	0.0	0.0	0.0	0.0
Lu(d)	1.7	5.8	5.7	1.2
N(tot)[a]	57.8	53.9	34.3	35.7
Si(p)[b]	0.0	0.0	3.1	2.1
Si(d)[b]	0.0	1.2	0.8	0.0

[a]Total for all three N atoms and for all N functions. [b]Total for all six Si atoms (only p and d functions).

(dispersion) interactions.[48] This is not meant to imply that attractive M···Si−C interactions do not exist in f-element $M[N(SiMe_3)_2]_3$ and $M[CH(SiMe_3)_2]_3$ complexes. Compelling arguments have been made for their presence in these compounds, both from high-level computational results and from reactivity considerations (e.g., decomposition of $Lu[N(SiMe_3)_2]_3$ under ALD conditions, even with H_2O as a reagent, always leads to Lu silicate films, a fact that has been attributed to the existence of Lu···Si interactions that help remove Si and Lu together from the compound during decomposition[49]).

A detailed DFT examination of the role of valence d orbitals in the geometry of the f-element $Sm[N(SiR_2Me)(SiR_3)]_3$ (R = Me, H) complexes has been previously reported, with particular attention given to the effect on the Sm−N distance, N−Sm−N angle, and the planarity of the $[N(SiMe_3)_2]^-$ ligand (the latter by removing the d functions from the basis set for the silicon atoms).[18] We undertook a similar study with the $M[N(SiMe_3)_2]_3$ (M = P−Bi) complexes, with a focus on the accessibility of d acceptor orbitals on the group 15 centers that could conceivably support M···Si−C interactions. Table 4 lists a selection of bond lengths, angles, and intramolecular contacts for the four main-group amido complexes, calculated both with and without valence d orbitals on the central atom (using the LANL08(d)[50] and LANL08[51] ECP basis sets on the central atoms, respectively, and the M06-L functional[52]). By way of generalization, it can be said that the inclusion of d polarization functions improves the reproduction of the M−N distances slightly; the effect is largest for P (0.04 Å shortening) but is essentially negligible for Sb and Bi (<0.01 Å change). The N−M−N angles display less alteration on the addition of d functions: that for P widens by 0.2°, but there is no effect in the Bi derivative. Nonbonded distances are consistently overestimated, by up to 0.2 Å in the case of the As···Si and As···C contacts; the addition of d functions does not change the As···C distance, and shortens the As···Si by only 0.01 Å. For P, the addition of a d function shortens the P···Si contact by 0.03 Å, but still leaves it 0.09 Å longer than the experimental value. In summary, at this level of theory the inclusion of d functions has small to negligible effects on the geometries of the $M[N(SiMe_3)_2]_3$ complexes. This is in contrast to their large influence on the calculated structure of $Sm[N(SiH_2Me)(SiH_3)]_3$, for example, in which the removal of the d function on the metal causes the Sm−N bond length to increase by 0.074 Å and the N−Sm−N angle to increase by 5.3°, leading to a nearly planar molecule (N−Sm−N = 119.4°).[18]

An analysis of the molecular orbitals in the group 15 and f-element $M[N(SiMe_3)_2]_3$ complexes illustrates the difference in the involvement of d orbitals in their bonding. To a first approximation, all the compounds can be regarded as possessing C_3 symmetry (this approximation is poorest for **1**, as the 17° variation in the inclination of the Si−N−Si′ planes to the N_3 plane attests). All four main group complexes and, for comparison, the f-element complex $Lu[N(SiMe_3)_2]_3$ were optimized at the BP86-D3(BJ)/TZV2P level, and the percent character of various frontier orbitals, determined with a standard Mulliken analysis, is listed in Table 5. For **1**−**4**, the HOMO contains significant p orbital character, reflecting the conventional lone pair on the central group 15 centers. On descending the column, the energy gap between the N 2p orbitals and the valence *n*p orbitals increases, and the ordering

dx.doi.org/10.1021/ic501232z | Inorg. Chem. 2014, 53, 9703−9714

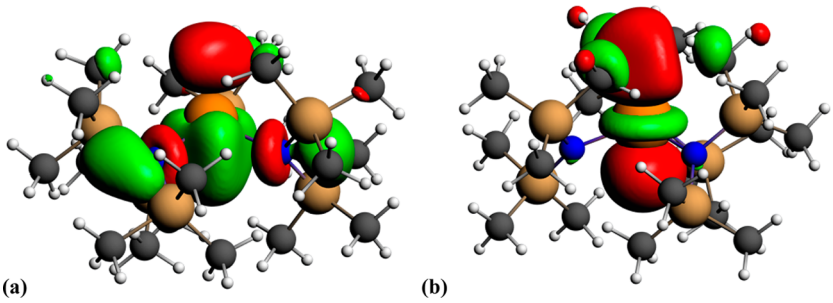

Figure 6. Depiction of the LUMO of $Sb[N(SiMe_3)_2]_3$ (a) and $Lu[N(SiMe_3)_2]_3$ (b). The Sb LUMO has 41% 5p character; the Lu is 53% $5d_{z^2}$.

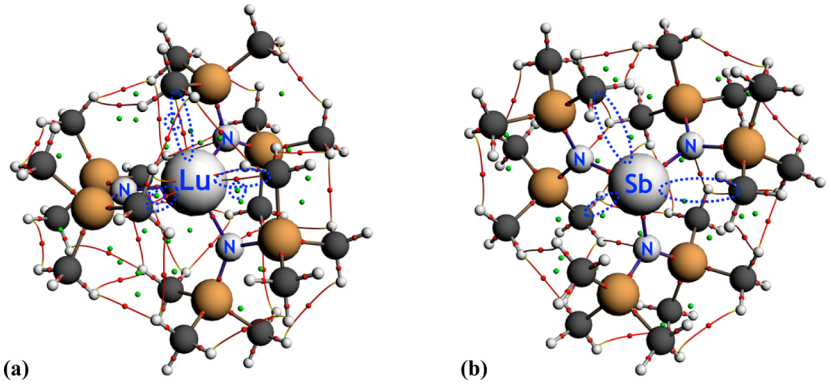

Figure 7. AIM representations for $Lu[N(SiMe_3)_2]_3$ (a) and $Sb[N(SiMe_3)_2]_3$ (b). Bond critical points are in red, and ring critical points are in green. In panel a, the bond critical paths from the γ-carbons to the metal are outlined with dashed ellipses; neighboring ring critical points are circled. The corresponding paths are absent in panel b; the ellipses outline the area where they would be expected to occur, were the interactions the same as in panel a.

of the energy levels and the extent of mixing changes. For complexes **2**−**4**, the energy gap is such that both the HOMO and next two frontier orbitals form a set (a + e symmetry) that contain significant N lone pair character as well and could potentially be involved in π-type bonding with the metal d orbitals. There is, however, almost negligible overlap with the metals' d orbitals in the main-group complexes (a maximum of 1.2% in **2**). In contrast, somewhat more d orbital involvement is apparent in the frontier orbitals in $Lu[N(SiMe_3)_2]_3$, which, however, largely represent the N lone pairs. The HOMO a-type orbital displays only a small amount of d orbital character (1.7% from the $5d_{z^2}$ orbital), but the e-type orbitals have 5.8% 5d orbital involvement.

The second set of frontier orbitals in **2**−**4** and $Lu[N(SiMe_3)_2]_3$ comprise M−N σ bonding orbitals (a + e), for which there is no measurable overlap with the d orbitals of the group 15 elements. This is consistent with the negligible change in M−N bond length in the calculated $M[N(SiMe_3)_2]_3$ structures in the absence of the d functions on the metal. In $Lu[N(SiMe_3)_2]_3$, the second e set lies slightly higher in energy than the a orbital, but together, they represent 6.9% overlap with the 5 d orbitals.

Attention should be given here to the orbitals in **1**; owing to its functionally lower symmetry than the other compounds, the four highest frontier orbitals are all singly degenerate and listed as HOMO − x in Table 5. The ordering is somewhat different from that in the heavier group 15 species, because the HOMO has more than twice the amount of p character (28%) than does that in the heavier analogues. The greater extent of P/N mixing also means that the N lone pairs are not as distinctly identifiable, and HOMO − (1−3) represent P−N σ bonding orbitals. As was found for the other main group complexes, however, the general comments above still apply as regards d orbital participation (i.e., negligible).

A final comment can be made about the LUMO in all the molecules. For **1**−**4**, there is no metal d character in the LUMOs. That for **3** is illustrated in Figure 6a; it consists only of various s and p orbitals (e.g., 40.9% 5p, 11.5% 5s, plus others). In contrast, more d orbital involvement is apparent in the LUMO of $Lu[N(SiMe_3)_2]_3$ (Figure 6b); the primary component (53.0%) is the $5d_{z^2}$ orbital; the second largest component (19.2%) is from the 6s orbital.

An alternative investigation of the possible importance of M···Si−C interactions in the group 15 complexes was conducted with Bader's atoms in molecules (AIM) theory.[53] Bond critical paths and points were calculated for **1**−**4** and $Lu[N(SiMe_3)_2]_3$, using the BP86-D3(BJ)/TZV2P optimized structures. Figure 7a illustrates the fact that three bond critical paths are clearly evident between the metal and the γ-C atoms in $Lu[N(SiMe_3)_2]_3$. The average electron density (in au) at the critical points along the paths is 0.018, 3 times the value for the points along the paths that represent van der Waals interactions between the methyl groups (e.g., the density of those in the triangle above the Lu atom average 0.0055 au); these are values appropriate for agostic-type interactions.[54] Ring critical points, which are indicative of electron delocalization in space, are associated with the Lu···C bond critical paths and are shifted toward the silicon atoms. In contrast, there are no bond critical paths or points between the group 15 elements and the β-Si or γ-C atoms in **1**−**4**. The diagram for $Sb[N(SiMe_3)_2]_3$ is shown in Figure 7b; that for the other three complexes looks essentially the same.

These results reinforce the supposition that the geometric distortions present in the group 15 $M[N(SiMe_3)_2]_3$ complexes

dx.doi.org/10.1021/ic501232z | Inorg. Chem. 2014, 53, 9703−9714

Table 6. Crystal Data and Summary of X-ray Data Collection

compound	$P[N(SiMe_3)_2]_3$ (**1**)	$As[N(SiMe_3)_2]_3$ (**2**)	$Sb[N(SiMe_3)_2]_3 \cdot {}^1/_2HN(SiMe_3)_2$ (**3**)
formula	$C_{18}H_{54}PN_3Si_6$	$C_{18}H_{54}AsN_3Si_6$	$C_{21}H_{63.5}SbN_{3.5}Si_7$
formula weight	512.13	556.10	683.63
cryst color	colorless	colorless	pale yellow
cryst dimens, mm^3	0.40 × 0.35 × 0.30	0.30 × 0.25 × 0.20	0.24 × 0.22 × 0.16
space group	$P\bar{1}$	$P2_1/c$	$P\bar{3}$
a, Å	8.9279(5)	8.4874(4)	16.0906(10)
b, Å	19.0519(10)	20.6151(9)	16.0906(10)
c, Å	20.6374(10)	18.2372(8)	8.4214(5)
α, deg	115.0854(12)	90	90
β, deg	97.9463(13)	93.2760(10)	90
γ, deg	95.3845(15)	90	120
vol, $Å^3$	3102.8(3)	3185.7(2)	1888.2(3)
Z	4	4	2
calcd density, Mg/m^3	1.096	1.159	1.202
abs coeff, mm^{-1}	0.331	1.303	0.968
$F(000)$	1128	1200	726
radiation type	Mo Kα (0.71073 Å)	Mo Kα (0.71073 Å)	Mo Kα (0.71073 Å)
temp, K	100(2)	100(2)	100.0(5)
limits of data collection	$2.15 \le \theta \le 26.38°$	$1.49 \le \theta \le 25.40°$	$2.42 \le \theta \le 33.72$
index ranges	$-11 \le h \le 11, -23 \le k \le 22, -14 \le l \le 25$	$-10 \le h \le 10, -24 \le k \le 24, -21 \le l \le 21$	$-25 \le h \le 12, -25 \le k \le 0, -13 \le l \le 13$
total reflns collected	34 673	23 641	37 098
unique reflns	12 599 (R_{int} = 0.0385)	5817 (R_{int} = 0.0353)	5043 (R_{int} = 0.0606)
transmission factors	0.8789–0.9072	0.6959–0.7806	0.6419–0.7467
data/restraints/params	12 599/0/561	5817/0/263	5043/77/157
R indices ($I > 2\sigma(I)$)	R_1 = 0.0422, wR_2 = 0.0967	R_1 = 0.0478, wR_2 = 0.1278	R_1 = 0.0596, wR_2 = 0.1522
R indices (all data)	R_1 = 0.0540, wR_2 = 0.1034	R_1 = 0.0591, wR_2 = 0.1368	R_1 = 0.0715, wR_2 = 0.1635
GOF on F^2	1.009	1.022	1.039
max/min peak in final diff map, $e^-/Å^3$	0.757/−0.554	0.927/−0.608	1.987/−0.990

are not the result of M···Si−C interactions or d-orbital involvement, but are the consequence of severe steric crowding. It therefore seems likely that similar geometric distortions that have sometimes been uncritically cited as diagnostic of M···Si−C interactions in f-element $M[(N,CH)(SiMe_3)_2]_3$ complexes are also sterically induced products of the crowded metal coordination environments in the complexes and that consequently the role of such intramolecular attractions on their geometries has been given more weight than is wholly warranted.

CONCLUSIONS

The three complexes $P[N(SiMe_3)_2]_3$, $As[N(SiMe_3)_2]_3$, and $Sb[N(SiMe_3)_2]_3$ complete the series of structurally authenticated group 15 tris(bistrimethylsilyl)amides; they are all pyramidal, monomeric species that exhibit disorder at the metal site. Collectively they display a notable resemblance to the f-element $M[N(SiMe_3)_2]_3$ (and $M[CH(SiMe_3)_2]_3$) counterparts, which are also pyramidal and display a pattern of bond length changes and intramolecular contacts that have been attributed to M···Si−C interactions.

Nevertheless, when three $-(N,CH)(SiMe_3)_2$ ligands are arranged around a central atom in a pyramidal manner (either because of polarization/d-orbital effects and possibly dispersion interactions (as with the f-element examples)[48,55] or because of near exclusive use of *n*p orbitals in the M−L bonding (in the group 15 cases)), the ligands will for steric reasons adopt conformations that distort the symmetrical $M-(N,CH)-(SiMe_3)_2$ linkages. The consequence will be the generation of small M−(N,CH)−Si and N−Si−C angles, and the placement of one or more of the carbon atoms close to the central atom. Such distortions are not observed in cases of planar $M[N(SiMe_3)_2]_3$ complexes (e.g., the group 13 (Al−Tl)[56] or transition metal (Ti, Mn, Fe, Co)[57] compounds), because the same amount of crowding is not present. Similar distortions are also not present in the less crowded $HAs[N(SiMe_3)_2]_2$,[9] even though the structure is pyramidal. In the absence of supporting spectroscopic (NMR, IR), computational, or reactivity evidence, considerable caution should be employed when relying solely on structural criteria to posit the existence of intramolecular agostic or related three-center bonding arrangements in low-coordinate but sterically congested metal complexes. As has been noted before, mere proximity is not a guaranteed marker of attractive interactions.[22]

EXPERIMENTAL SECTION

General Considerations. All manipulations were performed with the exclusion of air and moisture using high vacuum, Schlenk, or

dx.doi.org/10.1021/ic501232z | Inorg. Chem. 2014, 53, 9703−9714

glovebox techniques. Proton and carbon ($^{13}C\{^1H\}$) NMR spectra were obtained on a Bruker DRX-500 or DRX-400 spectrometer at 500 or 400 (^1H) and 100.1 (^{13}C) MHz and were referenced to the residual proton and ^{13}C resonances of C_6D_6 or THF-d_8. Elemental analysis was performed by ALS, Tucson, AZ.

Materials. AsI_3 as purchased from Aldrich and was visibly contaminated with purple iodine crystals. It was subsequently rinsed with hexane and the remaining dark orange solid was dried under vacuum and used without further purification. $K[N(SiMe)_2]$ and PCl_3 were purchased from commercial suppliers and used as received. Toluene and hexanes were distilled under nitrogen from potassium benzophenone ketyl.[58] Anhydrous THF was stored over molecular sieves. C_6D_6 was vacuum distilled from Na/K (22/78) alloy and stored over type 4A molecular sieves prior to use. $Sb[N(SiMe_3)_2]_3$ was synthesized by halide metathesis following the literature procedure,[6] using $K[N(SiMe_3)_2]$ in place of $Li[N(SiMe_3)_2]$.

Synthesis of $P[N(SiMe_3)_2]_3$ (1). $K[N(SiMe_3)_2]$ (2.31 g, 11.6 mmol) was dissolved in THF (70 mL). To this, PCl_3 (0.529 g, 3.85 mmol) was added dropwise over the course of 5 min at room temperature. After 1.5 h of stirring, the yellow suspension was filtered over a medium porosity frit. All volatiles were removed from the yellow filtrate to afford **1** as a waxy yellow solid (1.43 g, 72%). Colorless X-ray quality crystals were obtained by slow evaporation of a hexane solution of **1**. Anal. Calcd (%) for $C_{18}H_{54}N_3PSi_6$: C, 42.22; H, 10.63; N, 8.20; P, 6.05. Found (average of two determinations): C, 37.21; H, 8.96; N, 7.48, P, 5.40. Although all the values are low, their molar ratios are $C_{17.8}H_{51.0}N_{3.1}P_{1.0}$, close to the expected values.[59] ^1H NMR (400 MHz, C_6H_6, 298 K): δ 0.42. $^{13}C\{^1H\}$ NMR (100 MHz, C_6D_6, 298 K): δ 6.86. ^{31}P NMR (162 MHz, C_6H_6, 298 K): δ 136.0.

Synthesis of $As[N(SiMe_3)_2]_3$ (2). AsI_3 (0.503 g, 1.10 mmol) was dissolved in toluene (70 mL). To this, a solution of $K[N(SiMe)_2]$ in toluene (0.661 g, 3.31 mmol) was added dropwise over the course of 5 min at room temperature. After 1.5 h of stirring, the yellow suspension was filtered over a medium porosity frit. All volatiles were removed from the yellow filtrate to afford **2** as a waxy yellow solid (0.507 g, 83%). Colorless X-ray quality crystals were obtained by slow evaporation of a hexane solution of **2**. Anal. Calcd (%) for $C_{18}H_{54}AsN_3Si_6$: C, 38.88; H, 9.79; As, 13.47; N, 7.56. Found: C, 38.64; H, 9.08; As, 13.4; N, 7.15. ^1H NMR (400 MHz, C_6H_6, 298 K): δ 0.36 (500 MHz, THF-d_8, 298 K): δ 0.36 (δ 0.35 at 230 K). $^{13}C\{^1H\}$ NMR (100 MHz, C_6D_6, 298 K): δ 5.51.

General Procedures for X-ray Crystallography. A suitable crystal of each sample was located, attached to a glass fiber, and mounted on a Bruker diffractometer for data collection at 173(2) K or 100(2) K. Data collection and structure solutions for all molecules were conducted at the University of California, San Diego by Dr. Arnold L. Rheingold (P, As) or at the X-ray Crystallography Facility at the University of Rochester by Dr. William W. Brennessel (Sb). The intensity data were corrected for absorption and decay (SADABS). All calculations were performed using the current SHELXTL suite of programs.[60] Final cell constants were calculated from a set of strong reflections measured during the actual data collection. Relevant crystal and data collection parameters for each of the compounds are given in Table 6.

The space groups were determined based on systematic absences and intensity statistics. Compound **3** refined as a two-component twin, with a merohedral twin law of [0 $\bar{1}$ 0/$\bar{1}$ 0 0/0 0 $\bar{1}$]. For all the compounds, a direct-methods solution was calculated that provided most of the non-hydrogen atoms from the E-map. Several full-matrix least-squares/difference Fourier cycles were performed that located the remainder of the non-hydrogen atoms. Non-hydrogen atoms were refined with anisotropic displacement parameters. All hydrogen atoms were placed in ideal positions and refined as riding atoms with relative isotropic displacement parameters. In the case of **3**, there are two large peaks of electron density that remain in the final difference map. They are located 0.80 and 1.03 Å from atoms Si1 and Si2, respectively. They are separated by 2.97 Å, which is similar to the distance between Si1 and Si2 (3.02 Å). However, no methyl groups could be placed on these potential silicon atoms without violating the van der Waals space of neighboring symmetry equivalent methyl groups. Therefore, these peaks were left unassigned.

Note on Crystal Formation for 3. Compound **3** was initially isolated from hexanes solution as a yellow solid but not in the form of crystallographically useful crystals. A sample of **3** that had been stored in a glovebox for more than a year was later found to contain crystals suitable for data collection. One-half of a molecule of $HN(SiMe_3)_2$ was found per molecule of **3** in the lattice. The $HN(SiMe_3)_2$ molecule was found to be disordered over a crystallographic $\bar{3}$ site and is well separated from **3** (Me···Me′ contacts >4.0 Å). Evidently during the long storage, the compound was exposed to trace amounts of water that caused partial hydrolysis of the sample, which then aided crystallization. As a check on this, a mixture of freshly prepared $Sb[N(SiMe_3)_2]_3$ and $HN(SiMe_3)_2$ was allowed to slowly evaporate, and pale yellow plates formed within 1 week. The crystals were found to have the same unit cell as compound **3**.

Computational Details. Molecular mechanics calculations were performed with the UFF force field[45] as implemented in Gaussian 09.[61] In the case of $Ce[CH(SiMe_3)_2]_3$, charges were assigned to all atoms using the QEq method;[62] use of an alternative charge assignment method[63] was required to achieve convergence with $Sb[N(SiMe_3)_2]_3$. Assigning charges did not improve the structure of $Pu[N(SiMe_3)_2]_3$ (e.g., the overpyramidalization was worse), and they were not included in the final optimization. The Solid-G program[36] was used to compute ligand solid angles. They are converted to percentages (*G*-values) that reflect the shielding by each ligand of the central metal.

Density functional calculations were performed both with the Gaussian 09W[61] and with the Amsterdam Density Functional (ADF)[64] suite of programs. With Gaussian, the meta-GGA functional M06-L[52] was used; this provides an accounting for dispersion interactions. The effective core potential basis sets LANL08 were used for on all the metal centers when d functions were not desired; the corresponding LANL08(d) bases were used to incorporate additional polarization and diffuse functions.[65] The split valence polarized basis sets def2SVP were used for all other atoms.[66] With ADF, the functional BP86-D3(BJ) was used; it incorporates dispersion corrections according to Grimme's DFT-D3 method[67] and uses the Becke−Johnson damping function as well.[68] Full geometry optimizations were carried out with all-electron valence triple-ζ Slater-type basis sets with double-polarization functions for all atoms (TZ2P) from the ADF basis set library; ZORA scalar relativistic corrections were used for the Sb, Bi, and Lu complexes. The AIM analysis and Mulliken population analysis were conducted with the functionality built into the ADF program.

■ ASSOCIATED CONTENT

Supporting Information

CIF files for **1**−**3** and coordinates of the geometry optimized structures (.xyz format). This material is available free of charge via the Internet at http://pubs.acs.org.

■ AUTHOR INFORMATION

Corresponding Author

*Author e-mail address: t.hanusa@vanderbilt.edu.

Notes

The authors declare no competing financial interest.

■ ACKNOWLEDGMENTS

Financial support by the National Science Foundation (Grant CHE-1112181) is gratefully acknowledged. The constructive comments of a reviewer are appreciated.

■ REFERENCES

(1) Lappert, M. F.; Protchenko, A.; Power, P. P.; Seeber, A. *Metal Amide Chemistry*; Wiley: Wiltshire, England, 2009.

(2) Eller, P. G.; Bradley, D. C.; Hursthouse, M. B.; Meek, D. W. *Coord. Chem. Rev.* **1977**, *24*, 1−95. Anwander, R. *Top. Curr. Chem.* **1996**, *179*, 33−112.
(3) Chmely, S. C.; Hanusa, T. P.; Rheingold, A. L. *Organometallics* **2010**, *29*, 5551−5557.
(4) Vehkamäki, M.; Hatanpää, T.; Ritala, M.; Leskelä, M. *J. Mater. Chem.* **2004**, *14*, 3191−3197.
(5) Evans, W. J.; Rego, D. B.; Ziller, J. W. *Inorg. Chim. Acta* **2007**, *360*, 1349−1353.
(6) Liu, W.; Chang, A. Y.; Schaller, R. D.; Talapin, D. V. *J. Am. Chem. Soc.* **2012**, *134*, 20258−20261.
(7) (a) Kim, C.-K.; Khang, Y.-H.; Lee, T.-Y. Phase-change random access memory and method of manufacturing the same. U.S. Pat. Appl. 20090050869, 2009. (b) Shin, W.-C.; Khang, Y.-H. Method of forming phase change material thin film, and simplified method of manufacturing phase change memory device using the same with improved memory characteristics. Eur. Pat. Appl. 1806427, 2007. (c) Lee, J.-H.; Park, Y.-S.; Park, S.-H. Hexa(trimethylsilyl) antimony triamine precursor for manufacture of Ge2-Sb2-Te5 phase-change films for RAM memory devices. U.S. Pat. Appl. 20060049447, 2006;. (d) Seo, B.-S.; Lee, J.-H. Ge precursor, Ge-Sb-Te thin layer, phase-change memory device. Eur. Pat. Appl. 1675194, 2006.
(8) Bochmann, M.; Song, X.; Hursthouse, M. B.; Karaulov, A. *J. Chem. Soc., Dalton Trans.* **1995**, 1649−1652.
(9) Olmstead, M. M.; Power, P. P.; Sigel, G. A. *Inorg. Chem.* **1988**, *27*, 2045−2049.
(10) Gynane, M. J. S.; Hudson, A.; Lappert, M. F.; Power, P. P.; Goldwhite, H. *J. Chem. Soc., Dalton Trans.* **1980**, 2428−2433.
(11) Michalik, D.; Schulz, A.; Villinger, A. *Inorg. Chem.* **2008**, *47*, 11798−11806.
(12) Flynn, K. M.; Murray, B. D.; Olmstead, M. M.; Power, P. P. *J. Am. Chem. Soc.* **1983**, *105*, 7460−7461.
(13) Avtomonov, E. V.; Megges, K.; Li, X.; Lorberth, J.; Wocadlo, S.; Massa, W.; Harms, K.; Churakov, A. V.; Howard, J. A. K. *J. Organomet. Chem.* **1997**, *544*, 79−89.
(14) Hering, C.; Schulz, A.; Villinger, A. *Angew. Chem., Int. Ed.* **2012**, *51*, 6241−6245.
(15) Pohl, S.; Krebs, B. *Chem. Ber.* **1977**, *110*, 3183−3189.
(16) Appel, R.; Gudat, D.; Niecke, E.; Nieger, M.; Porz, C.; Westermann, H. *Z. Naturforsch., B: Chem. Sci.* **1991**, *46*, 865−83.
(17) Perrin, L.; Maron, L.; Eisenstein, O.; Lappert, M. F. *New J. Chem.* **2003**, *27*, 121−127.
(18) Brady, E. D.; Clark, D. L.; Gordon, J. C.; Hay, P. J.; Keogh, D. W.; Poli, R.; Scott, B. L.; Watkin, J. G. *Inorg. Chem.* **2003**, *42*, 6682−6690.
(19) In much of the literature on the subject, M···Si−C interactions are often termed "agostic"; this term, however, properly and specifically refers only to three-center−two-electron M···H−C interactions. Brookhart, M.; Green, M. L. H. *J. Organomet. Chem.* **1983**, *250*, 395−408. We maintain this distinction here.
(20) (a) Cooper, A. C.; Clot, E.; Huffman, J. C.; Streib, W. E.; Maseras, F.; Eisenstein, O.; Caulton, K. G. *J. Am. Chem. Soc.* **1998**, *121*, 97−106. (b) Jaffart, J.; Cole, M. L.; Etienne, M.; Reinhold, M.; McGrady, J. E.; Maseras, F. *Dalton Trans.* **2003**, 4057−4064.
(21) (a) Ujaque, G.; Cooper, A. C.; Maseras, F.; Eisenstein, O.; Caulton, K. G. *J. Am. Chem. Soc.* **1998**, *120*, 361−365. (b) Clot, E.; Eisenstein, O. Agostic Interactions from a Computational Perspective: One Name, Many Interpretations. In *Principles and Applications of Density Functional Theory in Inorganic Chemistry II*; Kaltsoyannis, N., McGrady, J. E., Eds.; Springer: Berlin, Heidelberg, 2004; Vol. *113*, pp 1−36.
(22) Spicer, C. W.; Lovitt, C. F.; Girolami, G. S. *Organometallics* **2012**, *31*, 4894−4903.
(23) (a) Olshavsky, M. A.; Goldstein, A. N.; Alivisatos, A. P. *J. Am. Chem. Soc.* **1990**, *112*, 9438−9439. (b) Davidson, F. M.; Schricker, A. D.; Wiacek, R. J.; Korgel, B. A. *Adv. Mater.* **2004**, *16*, 646−649. (c) Dong, A.; Yu, H.; Wang, F.; Buhro, W. E. *J. Am. Chem. Soc.* **2008**, *130*, 5954−5961.
(24) Niecke, E.; Flick, W.; Pohl, S. *Angew. Chem., Int. Ed. Engl.* **1976**, *15*, 309−310.
(25) Cordero, B.; Gomez, V.; Platero-Prats, A. E.; Reves, M.; Echeverria, J.; Cremades, E.; Barragan, F.; Alvarez, S. *Dalton Trans.* **2008**, 2832−2838.
(26) The crystallographic results reported here are from a crystal that displayed merohedral twinning in a 60:40 ratio. Twinning need not be constant from crystal to crystal, and in fact is not in this case: examination of a second crystal revealed a twinning ratio of 68:32. Such variability does not affect any of the conclusions.
(27) F. Moser, D.; Schranz, I.; C. Gerrety, M.; Stahl, L.; J. Staples, R. *J. Chem. Soc., Dalton Trans.* **1999**, 751−758.
(28) Diel, B. N.; Huber, T. L.; Ambacher, W. G. *Heteroat. Chem.* **1999**, *10*, 423−429.
(29) Burford, N.; Macdonald, C. L. B.; Robertson, K. N.; Cameron, T. S. *Inorg. Chem.* **1996**, *35*, 4013−4016.
(30) Shutov, P. L.; Karlov, S. S.; Harms, K.; Sundermeyer, J.; Lorberth, J.; Zaitseva, G. S. *J. Fluorine Chem.* **2009**, *130*, 1017−1021.
(31) Westerhausen, M. *Coord. Chem. Rev.* **1998**, *176*, 157−210.
(32) Bartell, L. S.; Hirst, R. C. *J. Chem. Phys.* **1959**, *31*, 449−451.
(33) Jerzembeck, W.; Bürger, H.; Constantin, L.; Margulès, L.; Demaison, J.; Breidung, J.; Thiel, W. *Angew. Chem., Int. Ed.* **2002**, *41*, 2550−2552.
(34) Dunne, B. J.; Orpen, A. G. *Acta Crystallogr.* **1991**, *C47*, 345−347.
(35) Hawley, D. M.; Ferguson, G. *J. Chem. Soc. A* **1968**, 2059−2063.
(36) Guzei, I. A.; Wendt, M. *Dalton Trans.* **2006**, 3991−3999.
(37) Pauling, L. *The Nature of the Chemical Bond*, 3rd. ed.; Cornell University Press: Ithaca, NY, 1960; p 261.
(38) Brookhart, M.; Green, M. L. H.; Parkin, G. *Proc. Natl. Acad. Sci. U. S. A.* **2007**, *104*, 6908−6914.
(39) (a) Schaverien, C. J.; van der Heijden, H.; Orpen, A. G. *Polyhedron* **1989**, *8*, 1850−1852. (b) Van der Heijden, H.; Schaverien, C. J.; Orpen, A. G. *Organometallics* **1989**, *8*, 255−258. (c) Schaverien, C. J.; Nesbitt, G. J. *J. Chem. Soc., Dalton Trans.* **1992**, 157−167.
(40) Klooster, W. T.; Brammer, L.; Schaverien, C. J.; Budzelaar, P. H. M. *J. Am. Chem. Soc.* **1999**, *121*, 1381−1382.
(41) Maseras, F.; Crabtree, R. H. *Inorg. Chim. Acta* **2004**, *357*, 345−346. Maseras and Crabtree have argued that to be properly considered an agostic contact, two criteria must be met: (1) there must be an empty orbital that could overlap with the X−Y bond under consideration (generally associated with a distortion in the metal−ligand geometry), and (2) there must be evidence of weakening of the bond. The latter, they propose, is most easily accessible by calculation. This is especially true given the uncertainties in experimentally measured bond lengths, even when hydrogen is not involved. The $M[N(SiMe_3)_2]_3$ and $M[CH(SiMe_3)_2]_3$ complexes examined in this study illustrate the difficulty in establishing statistically significant bond lengthening from X-ray crystal structures. The difference between the length of the Si−Me bond that is oriented toward the metal versus the average of the other two on the $SiMe_3$ group (Δ_{SiC}) should be a positive number if lengthening (and hence weakening) is occurring. For the group 15 complexes, Δ_{SiC} is, in fact, either statistically indistinguishable from zero (owing to the esd of the Si−C bond lengths) or even slightly negative; that is, $\Delta_{SiC} = -0.017$ in the case of **2**. Lengthening is usually observed in the f-element $M[N(SiMe_3)_2]_3$ complexes; it is greatest in $Y[N(SiMe_3)_2]_3$ ($\Delta_{SiC} = +0.028$ Å), for example, and noticeable in $Sm[N(SiMe_3)_2]_3$·hexane (+0.013 Å) but less so in $Sm[N(SiMe_3)_2]_3$·THF (+0.005 Å, not significantly different from zero), demonstrating the influence of crystal packing effects on the value. Similarly small, insignificantly positive (or negative) values are found in other complexes, such as $U[N(SiMe_3)_2]_3$ (+0.005 Å) and $Er[N(SiMe_3)_2]_3$ (−0.006 Å). Consequently, the associated Si−C bond lengths are not listed in Table 1.
(42) Westerhausen, M.; Hartmann, M.; Schwarz, W. *Inorg. Chim. Acta* **1998**, *269*, 91−100.
(43) Avent, A. G.; Caro, C. F.; Hitchcock, P. B.; Lappert, M. F.; Li, Z.; Wei, X.-H. *Dalton Trans.* **2004**, 1567−1577.

(44) Sundermeyer, J.; Khvorost, A.; Harms, K. *Acta Crystallogr.* **2004**, *E60*, m1117−m1119.
(45) Rappé, A. K.; Casewit, C. J.; Colwell, K. S.; Goddard, W. A.; Skiff, W. M., III *J. Am. Chem. Soc.* **1992**, *114*, 10024−10035.
(46) Rappé, A. K.; Colwell, K. S.; Casewit, C. J. *Inorg. Chem.* **1993**, *32*, 3438−50.
(47) Pantazis, D. A.; McGrady, J. E.; Maseras, F.; Etienne, M. *J. Chem. Theory Comput.* **2007**, *3*, 1329−1336.
(48) How much distortion can be ascribed to attractive dispersion forces alone is not easily answered. In a limited test, we examined $Lu[N(SiMe_3)_2]_3$ with DFT methods, using both a "dispersion-free" functional (APF) and its dispersion-corrected counterpart (APF-D). The uncorrected APF functional (with Stuttgart RSC segmented/ECP on Lu, 6-31G(d,p) on the other atoms) actually performs quite well, with deviations in the Lu−N distances and N−Lu−N angles of 0.027 Å and 3.2°, respectively, from the experimental values. Distances to atoms not directly bonded to the metal are only slightly overestimated (e.g., Lu···C(H_3) by 0.05 Å). The dispersion correction contracts both bonded and non-bonded distances, so that the Lu−N distance is underestimated by 0.048 Å and the Lu···C(H_3) distance is now 0.03 Å shorter than the crystallographic value. The initial evidence suggests that purely dispersive effects in this molecule are comparatively small, but a survey of many additional compounds would be required to generalize the conclusion. Austin, A.; Petersson, G. A.; Frisch, M. J.; Dobek, F. J.; Scalmani, G.; Throssell, K. *J. Chem. Theory Comput.* **2012**, *8*, 4989−5007.
(49) Scarel, G.; Wiemer, C.; Fanciulli, M.; Fedushkin, I. L.; Fukin, G. K.; Domrachev, G. A.; Lebedinskii, Y.; Zenkevich, A.; Pavia, G. *Z. Anorg. Allg. Chem.* **2007**, *633*, 2097−2103.
(50) Check, C. E.; Faust, T. O.; Bailey, J. M.; Wright, B. J.; Gilbert, T. M.; Sunderlin, L. S. *J. Phys. Chem. A* **2001**, *105*, 8111−8116. By construction, the LANL08(d) basis sets for the group 15 elements also include an additional diffuse p function.
(51) Roy, L. E.; Hay, P. J.; Martin, R. L. *J. Chem. Theory Comput.* **2008**, *4*, 1029−1031.
(52) Zhao, Y.; Truhlar, D. G. *J. Chem. Phys.* **2006**, *125*, 194101−194118.
(53) Bader, R. F. W. *Atoms in Molecules: A Quantum Theory*; Oxford University Press: New York, 1994.
(54) Tognetti, V.; Joubert, L.; Raucoules, R.; De Bruin, T.; Adamo, C. *J. Phys. Chem. A* **2012**, *116*, 5472−5479.
(55) Perrin, L.; Maron, L.; Eisenstein, O. *Faraday Discuss.* **2003**, *124*, 25−39.
(56) (a) Tang, J. A.; Masuda, J. D.; Boyle, T. J.; Schurko, R. W. *ChemPhysChem* **2006**, *7*, 117−130. (b) Atwood, D. A.; Atwood, V. O.; Cowley, A. H.; Jones, R. A.; Atwood, J. L.; Bott, S. G. *Inorg. Chem.* **1994**, *33*, 3251−3254. (c) Petrie, M. A.; Ruhlandt-Senge, K.; Hope, H.; Power, P. P. *Bull. Soc. Chim. Fr.* **1993**, *130*, 851−5. (d) Allmann, R.; Henke, W.; Krommes, P.; Lorberth, J. *J. Organomet. Chem.* **1978**, *162*, 283−287.
(57) (a) Putzer, M. A.; Magull, J.; Goesmann, H.; Neumueller, B.; Dehnicke, K. *Chem. Ber.* **1996**, *129*, 1401−1405. Ellison, J. J.; Power, P. P.; Shoner, S. C. *J. Am. Chem. Soc.* **1989**, *111*, 8044−6. (b) Hursthouse, M. B.; Rodesiler, P. F. *J. Chem. Soc., Dalton Trans.* **1972**, 2100−2102.
(58) Perrin, D. D.; Armarego, W. L. F. *Purification of Laboratory Chemicals*, 3rd ed.; Pergamon: Oxford, 1988.
(59) (a) McCormick, M. J.; Sockwell, S. C.; Davies, C. E. H.; Hanusa, T. P.; Huffman, J. C. *Organometallics* **1989**, *8*, 2044−2049. (b) Meredith, M. B.; McMillen, C. H.; Goodman, J. T.; Hanusa, T. P. *Polyhedron* **2009**, *28*, 2355−2358.
(60) Lu, Y.; Kim, I. S.; Hassan, A.; Del, V.; David, J.; Krische, M. J. *Angew. Chem.* **2009**, *121*, 5118.
(61) Frisch, M. J.; Trucks, G. W.; Schlegel, H. B.; Scuseria, G. E.; Robb, M. A.; Cheeseman, J. R.; Scalmani, G.; Barone, V.; Mennucci, B.; Petersson, G. A.; Nakatsuji, H.; Caricato, M.; Li, X.; Hratchian, H. P.; Izmaylov, A. F.; Bloino, J.; Zheng, G.; Sonnenberg, J. L.; Hada, M.; Ehara, M.; Toyota, K.; Fukuda, R.; Hasegawa, J.; Ishida, M.; Nakajima, T.; Honda, Y.; Kitao, O.; Nakai, H.; Vreven, T.; Montgomery, J. A., Jr.; Peralta, J. E.; Ogliaro, F.; Bearpark, M.; Heyd, J. J.; Brothers, E.; Kudin, K. N.; Staroverov, V. N.; Kobayashi, R.; Normand, J.; Raghavachari, K.; Rendell, A.; Burant, J. C.; Iyengar, S. S.; Tomasi, J.; Cossi, M.; Rega, N.; Millam, J. M.; Klene, M.; Knox, J. E.; Cross, J. B.; Bakken, V.; Adamo, C.; Jaramillo, J.; Gomperts, R.; Stratmann, R. E.; Yazyev, O.; Austin, A. J.; Cammi, R.; Pomelli, C.; Ochterski, J. W.; Martin, R. L.; Morokuma, K.; Zakrzewski, V. G.; Voth, G. A.; Salvador, P.; Dannenberg, J. J.; Dapprich, S.; Daniels, A. D.; Farkas, O.; Foresman, J. B.; Ortiz, J. V.; Cioslowski, J.; Fox, D. J. *Gaussian 09*, revision D.01; Gaussian, Inc.: Wallingford, CT, 2009.
(62) Rappé, A. K.; Bormann-Rochotte, L. M.; Wiser, D. C.; Hart, J. R.; Pietsch, M. A.; Casewit, C. J.; Skiff, W. M. *Mol. Phys.* **2007**, *105*, 301−324.
(63) Rappé, A. K.; Goddard, W. A. *J. Phys. Chem.* **1991**, *95*, 3358−3363.
(64) ADF2013.01; SCM; Theoretical Chemistry; Vrije Universiteit; Amsterdam; The Netherlands, (http://www.scm.com).
(65) Schuchardt, K. L.; Didier, B. T.; Elsethagen, T.; Sun, L.; Gurumoorthi, V.; Chase, J.; Li, J.; Windus, T. L. *J. Chem. Inf. Model.* **2007**, *47*, 1045−1052.
(66) Weigend, F.; Ahlrichs, R. *Phys. Chem. Chem. Phys.* **2005**, *7*, 3297−3305.
(67) Grimme, S.; Antony, J.; Ehrlich, S.; Krieg, H. *J. Chem. Phys.* **2010**, *132*, No. 154104.
(68) Grimme, S.; Ehrlich, S.; Goerigk, L. *J. Comput. Chem.* **2011**, *32*, 1456−1465.
(69) Westerhausen, M.; Hartmann, M.; Pfitzner, A.; Schwarz, W. *Z. Anorg. Allg. Chem.* **1995**, *621*, 837−850.
(70) Rees, J.; William, S.; Just, O.; Van Derveer, D. S. *J. Mater. Chem.* **1999**, *9*, 249−252.
(71) Andersen, R. A.; Templeton, D. H.; Zalkin, A. *Inorg. Chem.* **1978**, *17*, 2317−2319.
(72) Sheng, E.-H.; Yang, G.-S.; Dong, B.-P. *Anhui Shifan Daxue Xuebao, Ziran Kexueban* **2002**, *25*, 254−256 (CAPLUS AN 2002:966063).
(73) Hitchcock, P. B.; Hulkes, A. G.; Lappert, M. F.; Li, Z. *Dalton Trans.* **2004**, 129−136.
(74) Herrmann, W. A.; Anwander, R.; Munck, F. C.; Scherer, W.; Dufaud, V.; Huber, N. W.; Artus, G. R. J. *Z. Naturforsch., B: Chem. Sci.* **1994**, *49*, 1789−1797.
(75) Niemeyer, M. *Z. Anorg. Allg. Chem.* **2002**, *628*, 647−657.
(76) Stewart, J. L.; Andersen, R. A. *Polyhedron* **1998**, *17*, 953−958.
(77) Gaunt, A. J.; Enriquez, A. E.; Reilly, S. D.; Scott, B. L.; Neu, M. P. *Inorg. Chem.* **2007**, *47*, 26−28.
(78) Ghotra, J. S.; Hursthouse, M. B.; Welch, A. J. *J. Chem. Soc., Chem. Commun.* **1973**, 669−670.
(79) Hitchcock, P. B.; Lappert, M. F.; Smith, R. G.; Bartlett, R. A.; Power, P. P. *J. Chem. Soc., Chem. Commun.* **1988**, 1007−1009.
(80) Van der Sluys, W. G.; Burns, C. J.; Sattelberger, A. P. *Organometallics* **1989**, *8*, 855−857.
(81) Murray, B.; Hvoslef, J.; Hope, H.; Power, P. P. *Inorg. Chem.* **1983**, *22*, 3421−3424.